

Proceedings

Reduction of Electrostatic Control Voltage with a Tri-Electrode Actuator †

Yu Zhou and Cyrus Shafai *

Department of Electrical and Computer Engineering, University of Manitoba, Winnipeg, MB R3T 5V6, Canada; umzhou73@myumanitoba.ca

* Correspondence: Cyrus.Shafai@umanitoba.ca; Tel.: +1-204-474-6302

† Presented at the Eurosensors 2017 Conference, Paris, France, 3–6 September 2017.

Published: 11 August 2017

Abstract: We present a new tri-electrode topology for reducing the control voltage for electrostatic actuators. Conventional parallel plate actuators are dual-electrode systems, formed by the MEMS structure and the drive electrode. By placing a perforated intermediate electrode between these elements, a tri-electrode configuration is formed. This topology enables a low voltage on the intermediate electrode to modulate the electrostatic force on the MEMS device, while the higher voltage on the drive electrode remains fixed. Results presented show that in comparison to conventional parallel plate electrostatic actuators, the intermediate electrode's modulating voltage can be as low as 20% of normal, while still providing the full actuation stroke.

Keywords: electrostatic actuator; tri-electrode topology; low voltage driving; FEM

1. Introduction

Conventional electrostatic actuators suffer pull-in after displacing only approximately 1/3 of the electrode separation [1], thereby limiting the controllable displacement range. Accordingly, the driver electrode must be placed distant from the MEMS structure when large controllable stroke is required. However, this leads to significantly elevated driving voltage, since the electrostatic force is proportional to the square of the separation distance. Various researches have been carried out [2–7] to overcome the drawback. Shai Shmulevich et al. [2] proposed a design with a nonlinear spring whose spring constant increases as the actuator closes, and an 18.6 μm out of 21 μm was achieved; Holger Conrad et al. [3] came up with a v-shaped actuator design so that the displacement is amplified by angle between the pulling direction and actuation direction. Other methods also exist such as nonlinear driver electrodes [4] and bi-directional moving of the upper electrode [5,6]. In [7], a capacitor in series with the electrode power supply was explored to avoid pull-in. However, this still suffers from the requirement for larger voltage as the series capacitor is charged in the effort to mitigate positive feedback of MEMS motion.

In this paper, we introduce an intermediate electrode between the underlying drive electrode and the above MEMS structure, to modulate the electrostatic force on the MEMS structure. Figure 1a shows a conventional electrostatic actuator, with the MEMS structure placed at a distance D above the drive electrode biased to V_D . The controllable stroke $D_{\text{pull-in}}$ occurring at $V_{\text{pull-in}}$ is approximately 1/3 of D . The tri-electrode topology is shown in Figure 1b. The perforated intermediate electrode has solid elements of width W_E spaced W_S apart, and electrode-spacing pitch $L = W_E + W_S$. It is located a distance D_1 below the MEMS structure and D_2 above the drive electrode (held at a fixed voltage V_P). A modulation voltage V_i is applied on the intermediate electrode.

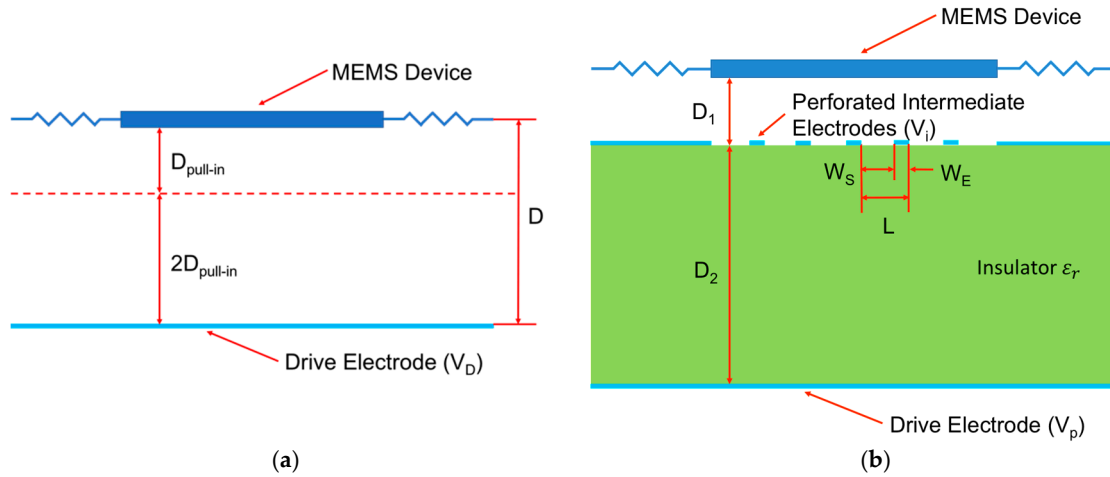


Figure 1. (a) Conventional electrostatic actuator; (b) New topology with perforated intermediate electrode.

The electric field modulation enabled by the intermediate electrode in the space D_1 is illustrated in the FEM simulation of Figure 2. This simulation has the MEMS held fixed. This figure shows the case of $W_S = D$, $W_E = 1/6 D$, $D_1 = 7/15 D$, and $D_2 = 7/10 \epsilon_r D$. In Figure 2a, a $V_i = -0.2 V_{pull-in}$ is applied on the intermediate electrode, while a $V_i = 0.2 V_{pull-in}$ is applied in Figure 2b. In both Figure 2a,b, the color gradient represents the potential, while the black arrow shows the electric field. It is clearly seen in Figure 2a that a large portion of the electric field converges on the intermediate electrode, while in Figure 2b the phenomenon is much less significant. The total induced charge on the surface of the MEMS also varies with V_i accordingly. Let us normalize the charge on the MEMS when $V_i = 0$ V as Q . For the case where $V_i = 0.2 V_{pull-in}$, the charge on the MEMS increases to $1.446 Q$. While for the case where $V_i = -0.2 V_{pull-in}$, the charge on the MEMS decreases to $0.554 Q$. This shows that a small fractional voltage V_i can cause a large change on the charge on the MEMS.

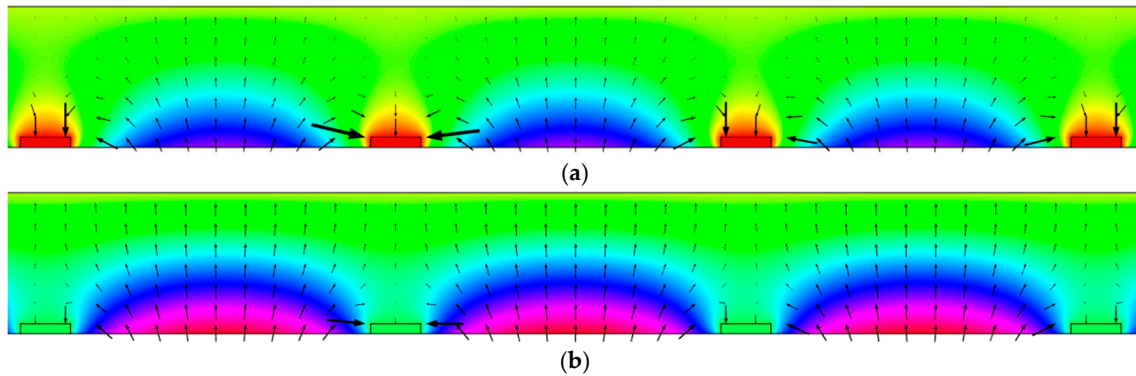


Figure 2. The electrical field distribution passing through intermediate electrode perforations: (a) Intermediate electrode voltage $V_i = -0.2 V_{pull-in}$; (b) Intermediate electrode voltage $V_i = 0.2 V_{pull-in}$.

2. Simulation Set-Up to Calculate MEMS Displacement

To demonstrate the theory of operation of the new tri-electrode topology, displacement studies were done for both cantilever and square membrane electrostatic actuators. These studies compared the performance of the tri-electrode actuator to that of conventional parallel plate *cantilever and membrane* actuators, see Figure 3. The dimensional parameters are given in Table 1 (see Figure 1 for parameter definition). For clarity, all parameters are normalized to D , which is the spacing between the drive electrode and the MEMS in the conventional situation.

Simulations of a conventional cantilever actuator were first carried out, in order to obtain the required driving voltage to achieve $D_{pull-in}$, and so $V_{pull-in}$. For the tri-electrode actuator simulations, first V_p has to be found such that it enables a similar stroke as $D_{pull-in}$. Simulations were done with $\pm V_i$

set to a fraction of $V_{pull-in}$, in order to find the needed drive electrode voltage (V_p) to achieve a maximum controllable stroke of approximately $D_{pull-in}$.

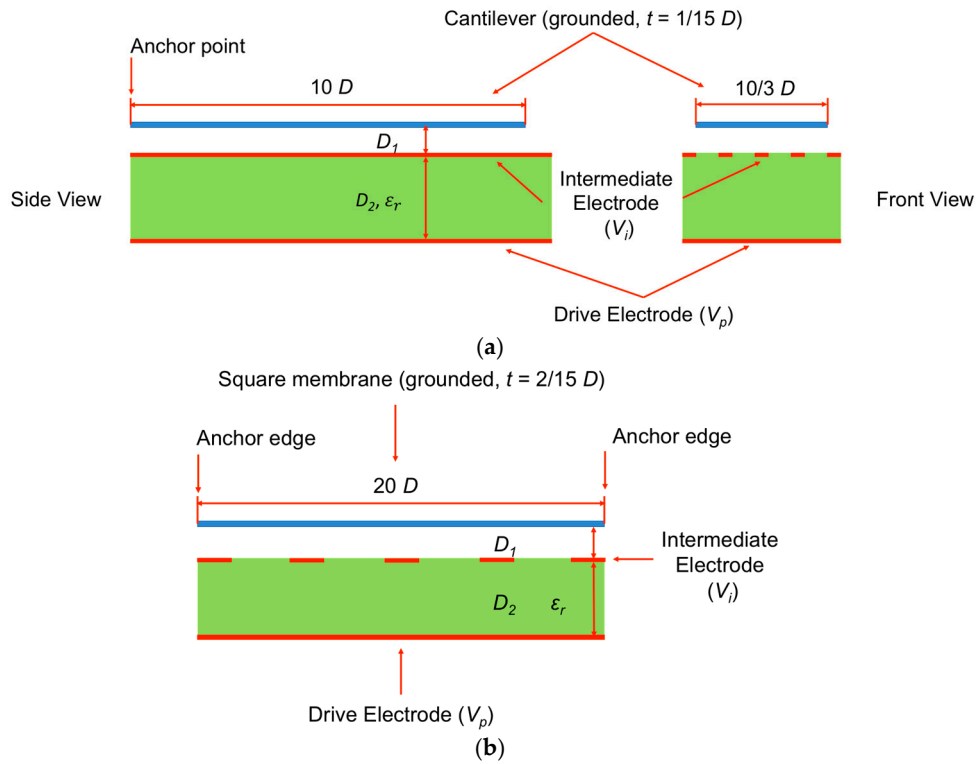


Figure 3. (a) Simulation structure of the cantilever actuator; (b) Structure of the square membrane actuator.

Table 1. Structure Parameters Used in Displacement Simulations.

Parameter	Cantilever Tri-Electrode Actuator	Membrane Tri-Electrode Actuator
L	$7/6 D$	$2/3 D$
W_s	D	$2/5 D$
W_E	$1/6 D$	$4/15 D$
D_1	$7/15 D$	$7/15 D$
D_2	$7/10 \epsilon_r D$	$14/15 \epsilon_r D$

3. MEMS Displacement Simulation Results

Figure 4a,b compare the tri-electrode topology to conventional parallel plate cantilever and membrane actuators. Displacement is plotted normalized to $D_{pull-in}$ for the conventional actuators. For the cantilever case, the same controllable stroke can be achieved using the tri-electrode topology with $-0.2 V_{pull-in} < V_i < 0.2 V_{pull-in}$. In the case of the square membrane, $-0.25 V_{pull-in} < V_i < 0.25 V_{pull-in}$ is required to realize the same controllable stroke. Also, with this topology, the controllable stroke can reach more than 80% of D_1 for the cantilever case, and more than 70% of D_1 for the square membrane case. This illustrates that the intermediate electrode does not suffer from pull-in for most of D_1 .

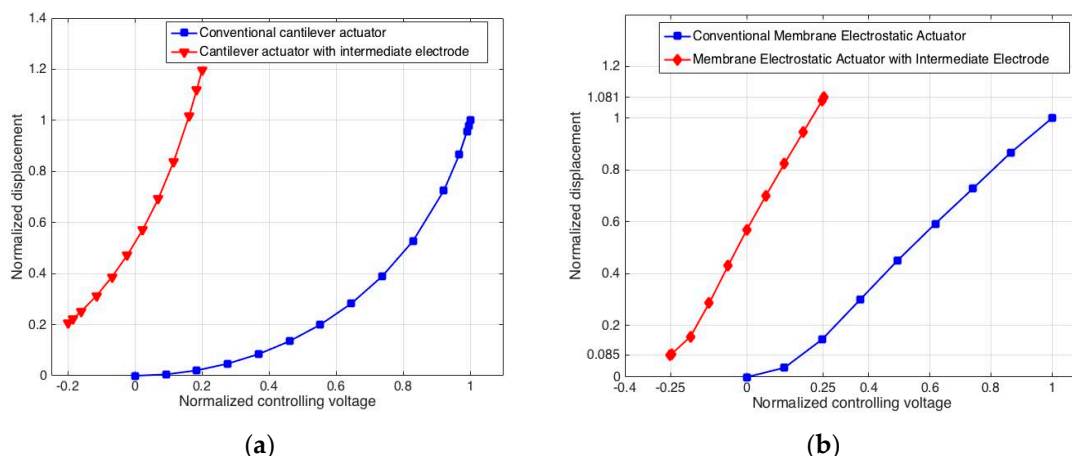


Figure 4. Simulations showing the tri-electrode topology achieving similar stroke as convention electrostatic actuators. (a) Cantilever simulation showing V_i needing to be only $-0.2 V_{pull-in} < V_i < 0.2 V_{pull-in}$; (b) Membrane simulation showing V_i needing to be only $-0.25 V_{pull-in} < V_i < 0.25 V_{pull-in}$.

4. Conclusions

In this paper, we introduce a tri-electrode topology for electrostatic actuators. This topology enables the same controllable stroke as conventional electrostatic actuators, but with greatly reduced control voltage. This is achieved by modulation of the electrostatic force on the MEMS structure by the variable control voltage on the perforated intermediate electrode, as opposed to the drive electrode which has a fixed voltage.

Acknowledgements: This research was financially supported by the Natural Sciences and Engineering Research Council (NSERC) of Canada, and the University of Manitoba Graduate Fellowship (UMGF).

Conflicts of Interest: The authors declare no conflict of interest.

References

1. Hung, E.S.; Senturia, S.D. Extending the travel range of analog-tuned electrostatic actuators. *J. Microelectromech. Syst.* **1999**, *8*, 497–505.
2. Shmulevich, S.; Rivlin, B.; Hotzen, I.; Elata, D. A gap-closing electrostatic actuator with a linear extended range. *J. Microelectromech. Syst.* **2013**, *22*, 1109–1114.
3. Conrad, H.; Schenk, H.; Kaiser, B.; Langa, S.; Gaudet, M.; Schimmanz, K.; Stolz, M.; Lenz, M. A small-gap electrostatic micro-actuator for large deflections. *Nat. Commun.* **2015**, doi:10.1038/ncomms10078.
4. Rosa, M.A.; de Bruyker, D.; Volkel, A.R.; Peeters, E.; Dunec, J. A novel external electrode configuration for the electrostatic actuation of MEMS based devices. *J. Micromech. Microeng.* **2004**, *14*, 446–451.
5. Sugimoto, T.; Nonaka, K.; Horenstein, M.N. Bidirectional electrostatic actuator operated with charge control. *J. Microelectromech. Syst.* **2005**, *14*, 718–724.
6. Ren, H.; Wang, W.; Tao, F.; Yao, J. A bi-directional out-of-plane actuator by electrostatic force. *Micromachines* **2013**, *4*, 431–443.
7. Seeger, J.I.; Crary, S.B. Analysis and simulation of MOS capacitor feedback for stabilizing electrostatically actuated mechanical devices. *Trans. Built Environ.* **1997**, *31*, doi:10.2495/MIC970201.

